Colloid Polym Sci 280: 207–217 (2002)
© Springer-Verlag 2002

ORIGINAL CONTRIBUTION

Augustín Amigó-Melchior
Heino Finkelmann

Lyotropic smectic layering of side-on polysoaps in water

Received: 21 May 2001
Accepted: 27 August 2001

A. Amigó-Melchior · H. Finkelmann (✉)
Institut für Makromolekulare Chemie
der Universität Freiburg
Stefan-Meier-Straße 31
79104 Freiburg, Germany
e-mail: finkelma@uni-freiburg.de

Abstract The synthesis and characterization of lyotropic smectic amphiphilic side-on polymers are described. The amphiphile consists of a rigid, aromatic core with two terminal ethyleneoxide chains of various lengths and is laterally attached to a polysiloxane backbone; the length of the spacer has also been varied. The phase behavior of the monomeric amphiphiles and side-on polymers are determined by polarizing microscopy and ^{2}H-NMR measurements. In water, most of the low molecular weight surfactants show restricted lyotropic properties, namely lyotropic smectic phases. The packing restriction of the amphiphiles is due to their geometric anisometry. All side-on polymers exhibit only lyotropic smectic phases. The phase regime of the polymer mesophase with respect to the monomers depends on the spacer length. In contrast to surfactants having a flexible hydrophobic group, these amphiphiles align spontaneously parallel to an external magnetic field, leading to perfect lyotropic smectic monodomains.

Keywords Lyotropic smectic amphiphilic side-on polymers · Polarizing microscopy · Deuterium nuclear magnetic resonance · Geometric anisometry · Spacer length

Introduction

Replacing the flexible hydrophobic part of an amphiphile with a rigid hydrophobic aromatic core yields rigid anisometric surfactant molecules [1–3]. The combination of an anisotropic shape (thermotropic mesogens) and amphiphilicity (lyotropic surfactants) causes packing restraints which only permit the formation of micelles having specific geometry [4]. Disc-like surfactants, initially synthesized by Boden et al., have been found to form micelles which rearrange into columnar phases [5] (see Fig. 1). Investigations reported by Schafheutle et al. on the phase behavior of low molecular-weight amphiphiles with rigid rod-like hydrophobic moieties reveal that liquid crystalline phases are all of the smectic type, regardless of the hydrophilic/hydrophobic balance (HLB) and temperature or concentration regimes [6].

By introducing polymerizable groups into monomeric amphiphiles, different types of polysurfactants can be realized, where the amphiphilic moiety is attached as a side-chain via the hydrophilic or hydrophobic end to the polymer backbone (polysoaps). Detailed investigations of binary phase diagrams of monomeric and polymeric surfactants in aqueous solution have proved that the polysoaps form liquid crystalline phases in water. The phase structure of the polymers is similar to the phase structure of conventional low molar mass lyotropic liquid crystals and the well-known polymorphism occurs. While for low molar mass surfactants in dilute solutions the association number N of associated amphiphiles is essentially determined by the hydrophobic-hydrophilic balance of the molecules, for polysurfactants, N is determined by the degree of polymerization r. Consequently when $r \geq N$ no critical micelle concentration occurs. Furthermore, the micellar

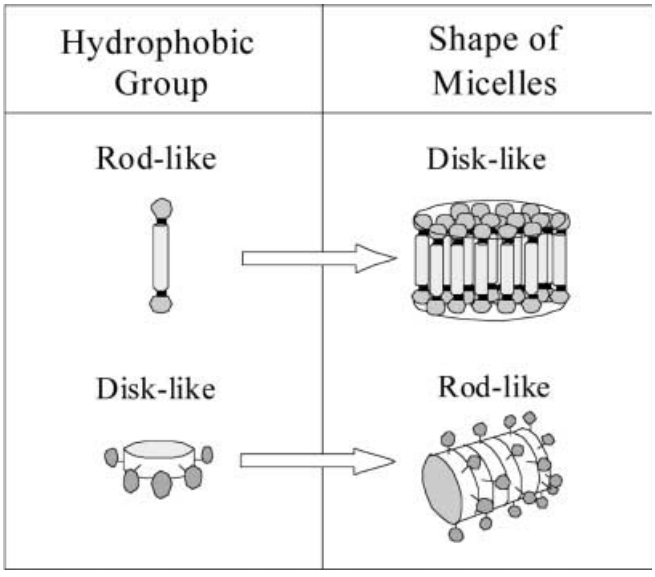

Fig. 1 Geometrical packing of anisometric surfactant molecules into anisometric micelles

shape becomes anisometric for $r > N$ in very dilute solutions, even if the monomer units tend to form spherical micelles. The restriction of motions of the amphiphiles, due to the linkage to the polymer main chain, leads to an increased stability of the polymeric mesophase, compared to the monomeric systems.

In this paper we describe the synthesis and phase behavior of new polysoaps made by rigid rod-like amphiphiles, that combine the anisometric geometry of the Schafheutle's systems with the polymeric properties of polysoaps.

Materials and methods

For our investigations we started from the model compounds given in Fig. 2. These rod-like amphiphiles are not polymerizable and have been previously synthesized by Schafheutle. In water, the lyotropic smectic phases exhibit a polymorphism (S_A and S_C) which is similar to the polymorphism of thermotropic smectic liquid crystals.

In order to realize analogous polymeric compounds, we have to modify the chemical constitution of the model compounds towards functional monomers. There are two possible approaches for attaching these surfactants to a hydrophobic polymer backbone: the first being the introduction of a polymerizable group located at the hydrophilic end. This method should yield amphiphilic end-on polysoaps with hinder hydration at the hydrophilic part attached to the polymer main chain. In order to maintain the HLB we chose a second approach: connecting the rigid rod-like amphiphiles to a polymer backbone via their hydrophobic parts yielding side-on polysoaps. This is possible by grafting a lateral olefinic spacer to the rigid aromatic core. The olefinic group allows the attachment of the amphiphiles to a polymethylsiloxane backbone via an addition reaction.

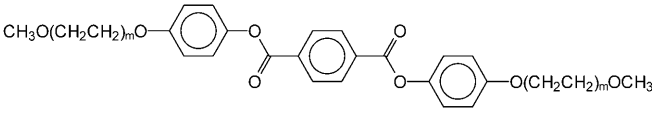

Fig. 2 Basic structure of Schafheutle's model compounds [6]

The variation of the length of the spacer and the hydrophilic oligo(ethylene glycol) allowed us to determine whether the HLB and the rigid/flexible balance influence the shape of the micelles and the domain of existence of the mesophase of the low molar mass surfactants. For this purpose, a homologous series of amphiphiles were synthesized.

The route for the synthesis of the new amphiphiles is presented schematically in Fig. 3. The monodisperse *p*-oligo(ethylene glycol)benzoic acids (Table 1) were prepared according to the synthetic route reported by Schafheutle [6]. The middle part of the rigid core was synthesized via azeotropic esterification of 2,5-dihydroxybenzoic acid and the 1-alkanols with *p*-toluenesulfonic acid as the catalyst.

Esterification of 1-(ω-alkylene) 2,5-dihydroxybenzoates by *p*-oligo(ethylene glycol)benzoic acid with *N,N′*-dicyclohexylcarbodiimide and 4-pyrrolidino-pyridine as catalyst yields the desired amphiphiles. All amphiphiles were purified by flash chromatography.

The polymeric amphiphiles (Table 2) were synthesized by polymer analogous reactions. The hydrosilation reaction between the precursor poly(methyl siloxane) ($P_n = 50$) and the amphiphilic olefins was catalyzed by a platinum catalyst.

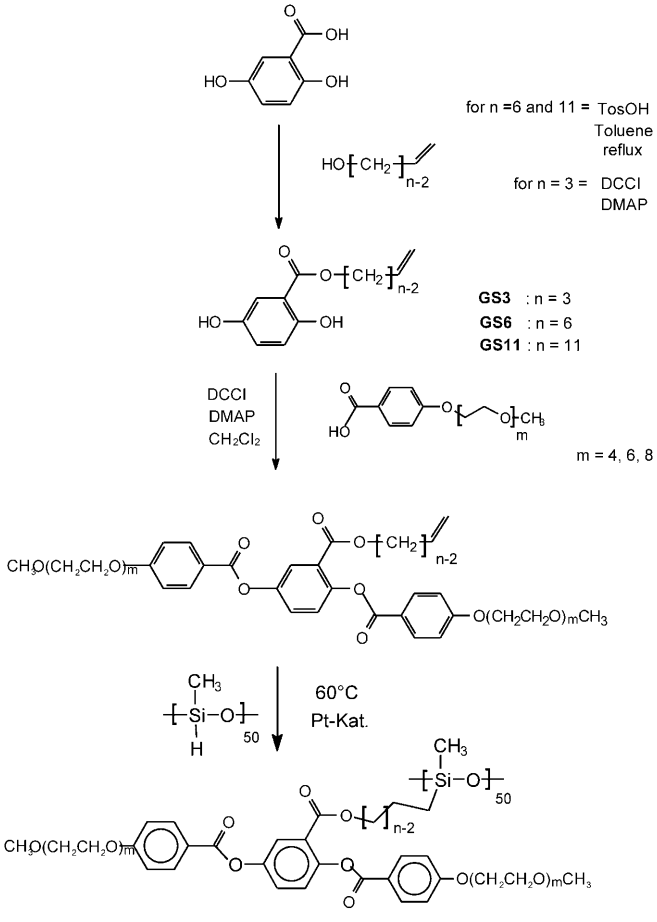

Fig. 3 Route for the synthesis of side-on amphiphilic polymers

Table 1 Homologous series of the monomeric surfactants

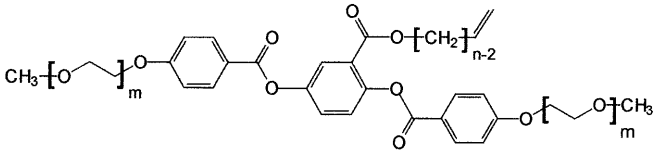

Monomer	m	n
M4GS3	4	3
M6GS3	6	3
M6GS6	6	6
M8GS6	8	6
M8GS11	8	11

Syntheses

Azeotropic esterification of 2,5 dihydroxybenzoic acid with alcohols The esters **GS6** and **GS11** were obtained by the following procedure: a mixture of 10 g (0.06 mol) of gentisinic acid, 25 ml of alcohol, and 0.5 g of *p*-toluenesulfonic acid in 150 ml of toluene was refluxed for 50 h in a Dean-Stark apparatus. The progress of the reaction was followed by TLC. When the gentisinic acid was no longer detectable, the solvent was removed under vacuum. Excess alcohol was removed by distillation. The residue was dissolved in 200 ml of diethylether, and this solution was extracted three times with 150 ml of saturated aqueous sodium bicarbonate. The organic layer was dried over magnesium sulfate. After removal of the solvent under vacuum a brown, viscous residue was obtained. After flash chromatography with diethylether/petroleum ether (1:1), the desired product was obtained [m.p.(**GS6**): 30–33 °C; yield: 75–80%].

^{1}H-NMR (**GS11**, 300 MHz, $CDCl_3$): δ7.25 (d, 1 Ar-H, $J=2$ Hz), δ7.0 (d, 1 Ar-H, $J=3$ Hz), δ6.8 (d, 1 Ar-H, $J=7$ Hz), δ5.8–5.6 ($CH_2=C\underline{H}$-), δ4.9 (dd, $C\underline{H}_2=CH$-), δ4.2 (t, O-$C\underline{H}_2$-CH_2-, $J=7$ Hz), δ1.7 (m, O-$C\underline{H}_2$-$C\underline{H}_2$-), δ1.4 (m, $CH_2=CH$-$C\underline{H}_2$-), δ1.2 (m, -$(CH_2)_6$-).

^{1}H-NMR (**GS6**, 300 MHz, $CDCl_3$): δ7.3 (d, 1 Ar-H, $J=2$ Hz), δ7.0 (d, 1 Ar-H, $J=3$ Hz), δ6.85 (d, 1 Ar-H, $J=9$ Hz), δ5.8–5.6 ($CH_2=C\underline{H}$-), δ4.9 (dd, $C\underline{H}_2=CH$-), δ4.3 (t, O-$C\underline{H}_2$-CH_2-, $J=7$ Hz), δ1.75 (m, OCH_2-$C\underline{H}_2$-), δ1.55 (m, $CH_2=CH$-$C\underline{H}_2$), δ1.4 (m, -CH_2-).

Table 2 Comparison of multiple myeloma (MM) and osteosclerotic myeloma

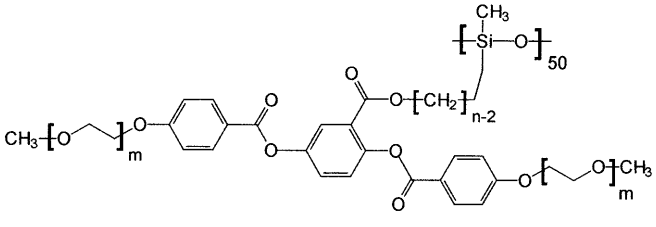

Polymer	m	n
P4GS3	4	3
P6GS3	6	3
P6GS6	6	6
P8GS11	8	11

Esterification of 2,5- dihydroxybenzoic acid with allyl alcohol. In a 250 ml round-bottom flask, 0.06 mol of 2,5 dihydroxybenzoic acid and 0.06 mol of 1,3 dicyclohexyl-carbodiimide were dissolved with 150 ml allyl alcohol. DMAP (0.1 mmol) was added and the solution was stirred for 48 h at room temperature. The allyl alcohol was removed by distillation. The residue was partially dissolved in 200 ml of CH_2Cl_2 and filtered. The solution was extracted twice with 50 ml saturated $NaHCO_3$. The organic phase was dried over magnesium sulfate and CH_2Cl_2 was removed under vacuum. The crude product was purified by flash chromatography with ether/petrol ether (1:1) (retention factor: 0.32) to obtain a white solid. The yield was 70%.

^{1}H-NMR (**GS3**, 300 MHz, $CDCl_3$): δ7.3 (d, 1 Ar-H, $J=2$ Hz), δ7.0 (d, 1 Ar-H, $J=3$ Hz), δ6.9 (d, 1 Ar-H, $J=9$ Hz), δ6.1–5.9 ($CH_2=C\underline{H}$-), δ5.45 (dd, $C\underline{H}_2=CH$-), δ4.9 (t, O-CH2-).

Preparation of the monomers All monomers were synthesized by the following procedure: 12 mmol **GS***n* ($n=$ **3**, **6**, **11**), 24 mmol M(4–5) *p*-oligo(ethylene glycol)benzoic acid, 0.1 mmol DMAP and 1,3- dicyclohexylcarbodiimide were dissolved in dry CH_2Cl_2. The solution was stirred at room temperature for 72 h, filtered, concentrated and dissolved in 100 ml ether. After the ether solution was washed with 50 ml of 5% acetic acid and 50 ml saturated $NaHCO_3$, it was then dried over magnesium sulfate and concentrated to yield the crude product. After flash chromatography with ether/acetone (1:1) the desired monomers were obtained as a colorless oil. The yield was 50–60%.

^{1}H-NMR (**M4GS3**, 300 MHz, $CDCl_3$): δ8.2 (d, 4 Ar-H, $J=10$ Hz), δ8.0 (d, 1 Ar-H, $J=2$ Hz), δ7.6 (d, 1 Ar-H, $J=6$ Hz), δ7.4 (d, 1 Ar-H, $J=9$ Hz), δ7.1 (d, 4 Ar-H, $J=10$ Hz), δ6.0–5.8 ($CH_2=C\underline{H}$-), δ5.3 (dd, $C\underline{H}_2=CH$-), δ4.75 (2H, COO-CH_2-), δ4.35 (t, 4H, Ar-O-CH_2-), δ4.0 (t, 4H, Ar-O-CH_2-$C\underline{H}_2$-), δ3.8–3.65 (m, 24H, O-CH_2-CH_2), δ3.5 (s, 6H, O-CH_3).

^{1}H-NMR (**M6GS3**, 300 MHz, $CDCl_3$): δ8.2 (d, 4 Ar-H, $J=10$ Hz), δ8.0 (d, 1 Ar-H, $J=2$ Hz), δ7.6 (d, 1 Ar-H, $J=6$ Hz), δ7.4 (d, 1 Ar-H, $J=9$ Hz), δ7.1 (d, 4 Ar-H, $J=10$ Hz), δ6.0–5.8 ($CH_2=C\underline{H}$-), δ5.3 (dd, $C\underline{H}_2=CH$-), δ4.75 (2H, COO-CH_2-), δ4.35 (t, 4H, Ar-O-CH_2-), δ4.0 (t, 4H, Ar-O-CH_2-$C\underline{H}_2$-), δ3.8–3.65 (m, 40H, O-CH_2-CH_2), δ3.5 (s, 6H, O-CH_3).

^{1}H-NMR (**M6GS6**, 300 MHz, $CDCl_3$): δ8.1 (d, 4 Ar-H, $J=10$ Hz), δ7.8 (d, 1 Ar-H, $J=2$ Hz), δ7.4 (d, 1 Ar-H, $J=6$ Hz), δ7.2 (d, 1 Ar-H, $J=9$ Hz), δ6.95 (d, 4 Ar-H, $J=10$ Hz), δ5.7–5.55 ($CH_2=C\underline{H}$-), δ4.9 (dd, $C\underline{H}_2=CH$-), δ4.2 (4H, Ar-O-CH_2-), δ4.1 (t, COO-CH_2-), δ3.8 (t, 4H, Ar-O-CH_2-$C\underline{H}_2$-), δ3.7–3.5 (m, 40H, O-CH_2-CH_2), δ3.3 (s, 6H, O-CH_3), δ1.9 (2H, COO-CH_2-$C\underline{H}_2$-), δ1.45 (2H, $CH_2=CH$-$C\underline{H}_2$), δ1.3(2H, -CH_2-$C\underline{H}_2$-CH_2-).

^{1}H-NMR (**M8GS6**, 300 MHz, $CDCl_3$): δ8.1 (d, 4 Ar-H, $J=10$ Hz), δ7.8 (d, 1 Ar-H, $J=2$ Hz), δ7.4 (d, 1 Ar-H, $J=6$ Hz), δ7.2 (d, 1 Ar-H, $J=9$ Hz), δ6.95 (d, 4 Ar-H, $J=10$ Hz), δ5.7–5.55 ($CH_2=C\underline{H}$-), δ4.9 (dd, $C\underline{H}_2=CH$-), δ4.2 (4H, Ar-O-CH_2-), δ4.1 (t, COO-CH_2-), δ3.8 (t, 4H, Ar-O-CH_2-$C\underline{H}_2$-), δ3.7–3.5 (m, 56H, O-CH_2-CH_2), δ3.3 (s, 6H, O-CH_3), δ1.9 (2H, COO-CH_2-$C\underline{H}_2$-), δ1.45 (2H, $CH_2=CH$-$C\underline{H}_2$), δ1.3(2H, -CH_2-$C\underline{H}_2$-CH_2-).

^{1}H-NMR (**M8GS11**, 300 MHz, $CDCl_3$): δ8.1 (d, 4 Ar-H, $J=10$ Hz), δ7.8 (d, 1 Ar-H, $J=2$ Hz), δ7.4 (d, 1 Ar-H, $J=6$ Hz), δ7.2 (d, 1 Ar-H, $J=9$ Hz), δ6.95 (d, 4 Ar-H, $J=10$ Hz), δ5.7–5.55 ($CH_2=C\underline{H}$-), δ4.9 (dd, $C\underline{H}_2=CH$-), δ4.2 (4H, Ar-O-CH_2), δ4.1 (t, COO-CH_2-), δ3.8 (t, 4H, Ar-O-CH_2-$C\underline{H}_2$-), δ3.7–3.5 (m, 56H, O-CH_2-CH_2), δ3.3 (s, 6H, O-CH_3), δ1.75 (m, COO-CH_2-$C\underline{H}_2$-), δ1.4 (m, $CH_2=CH$-$C\underline{H}_2$), δ1.2 (m, -$(CH_2)_6$-).

Preparation of the polymers The monomeric amphiphile (5–10% excess) and poly[oxy(methylsilylene)] were dissolved in toluene and 150 ppm Pt catalyst (Wacker SLM 86003) was added. The solution was left under an atmosphere of dry nitrogen for 3 days at 60 °C. The reaction was monitored by IR spectroscopy where the disappearance of the Si-H absorption band at 2175 cm^{-1} indicated

complete conversion. The polymers were precipitated several times from toluene in hexane until no monomer could be detected by thin layer chromatography. The yields were 60–75%.

^{1}H-NMR($\mathbf{P_mGS_{n\text{-}2}}$, 300 MHz, $CDCl_3$): δ0.1–0.3 (-Si-CH_3), δ0.4–0.9 (-Si-CH_2-R).

Excepting the olefinic peaks, all the other peaks correspond to the monomer spectra with the typical broadening of polymer peaks.

Measurements

Optical microscopy All microscopic investigations were carried out with a Leitz-Ortholux II Poll-BK microscope equipped with a modified Mettler FP 80/82 hotstage, which can be cooled with liquid nitrogen. Samples with different concentrations were prepared using an analytical balance and mixed in Teflon capsules on a vibrating mill. All points of the phase transitions in the phase diagram were determined by heating the samples. Penetration technique experiments were performed to obtain initial information on the phase behavior, including all temperature minima and maxima of the liquid crystalline phases.

NMR measurements The ^{2}H-NMR spectra were recorded on a Bruker MSL 300 at a frequency of 46.073 MHz. The sample temperature was kept constant to ± 1 K by a Eurotherm. The measurements at various angles to the magnetic field were performed using a goniometer probe with a 5 mm solenoid coil. The sample tube can be rotated about its long axis, which is perpendicular to the external magnetic field. The samples were aligned in the magnet by slow cooling from the isotropic phase and subsequent annealing in the biphasic region. Once the temperature is lowered to the pure mesophase region, samples can be rotated over a period of some hours in the magnetic field without realignment of the directors.

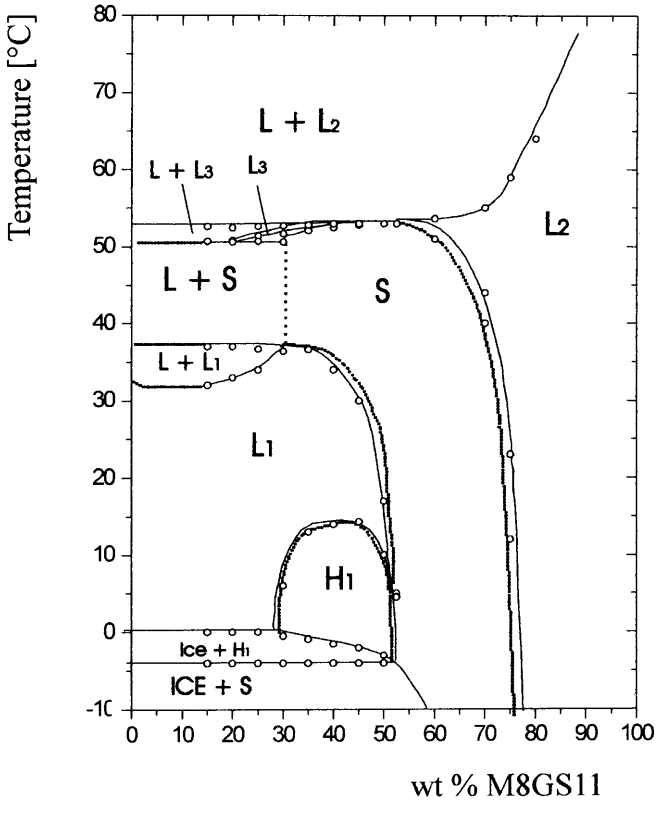

Fig. 4 Phase diagram of M8GS11 in water

Results and discussion

Before describing the phase behavior of the monomers and polymers, some general properties of the synthesized compounds should be considered. All monomers have the same rigid basic structure, namely an aromatic core made by two benzoic and one hydroquinone ring, and possess a positive anisotropy of the diamagnetical susceptibility. Due to the variations of spacer- and

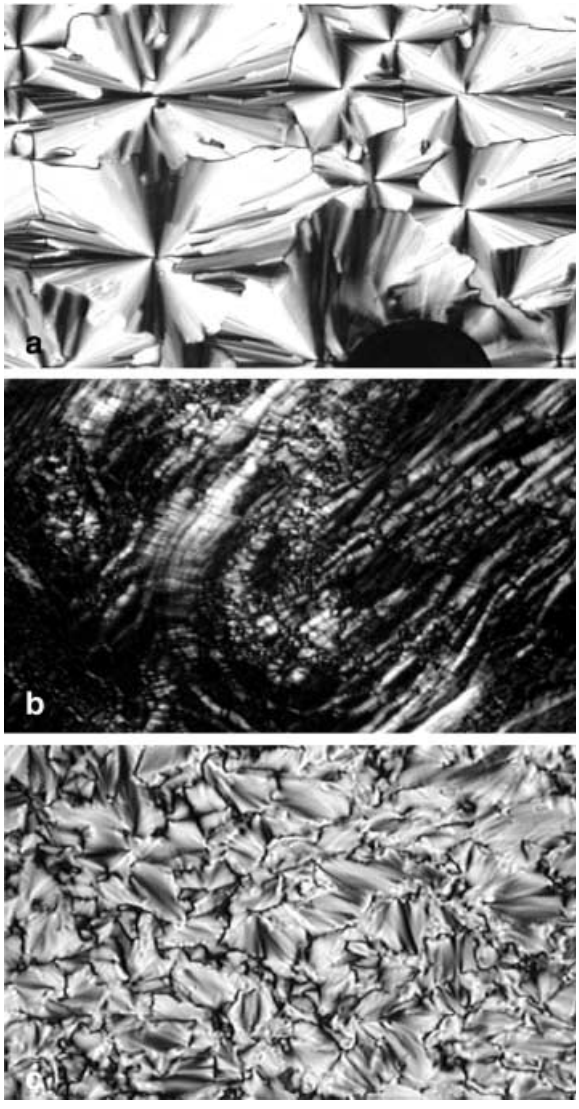

Fig. 5 a Hexagonal fan shaped texture of M8GS11 at 40% (w/w) and 13 °C. **b** Homeotropic lamellar texture with oily streaks of M8GS11 at 55% (w/w) and 35 °C. **c** S_A focal conic texture of M8GS11 at 70% (w/w) and 24 °C

oligo(ethylene glycol) chain length, the systems can be distinguished in their flexibility and HLB.

The molecular flexibility and HLB are therefore the main properties that should be considered for the comparative studies of the phase behavior of the present low molar mass homologous series.

In addition, the resulting polymers belong to a new class of polysoaps, having a chemical constitution similar to that of classical thermotropic side-on polymers. The chemical structure/phase behavior relationship of side-on liquid crystalline polymers has been studied intensively [8–15]. Attaching the mesogen later-

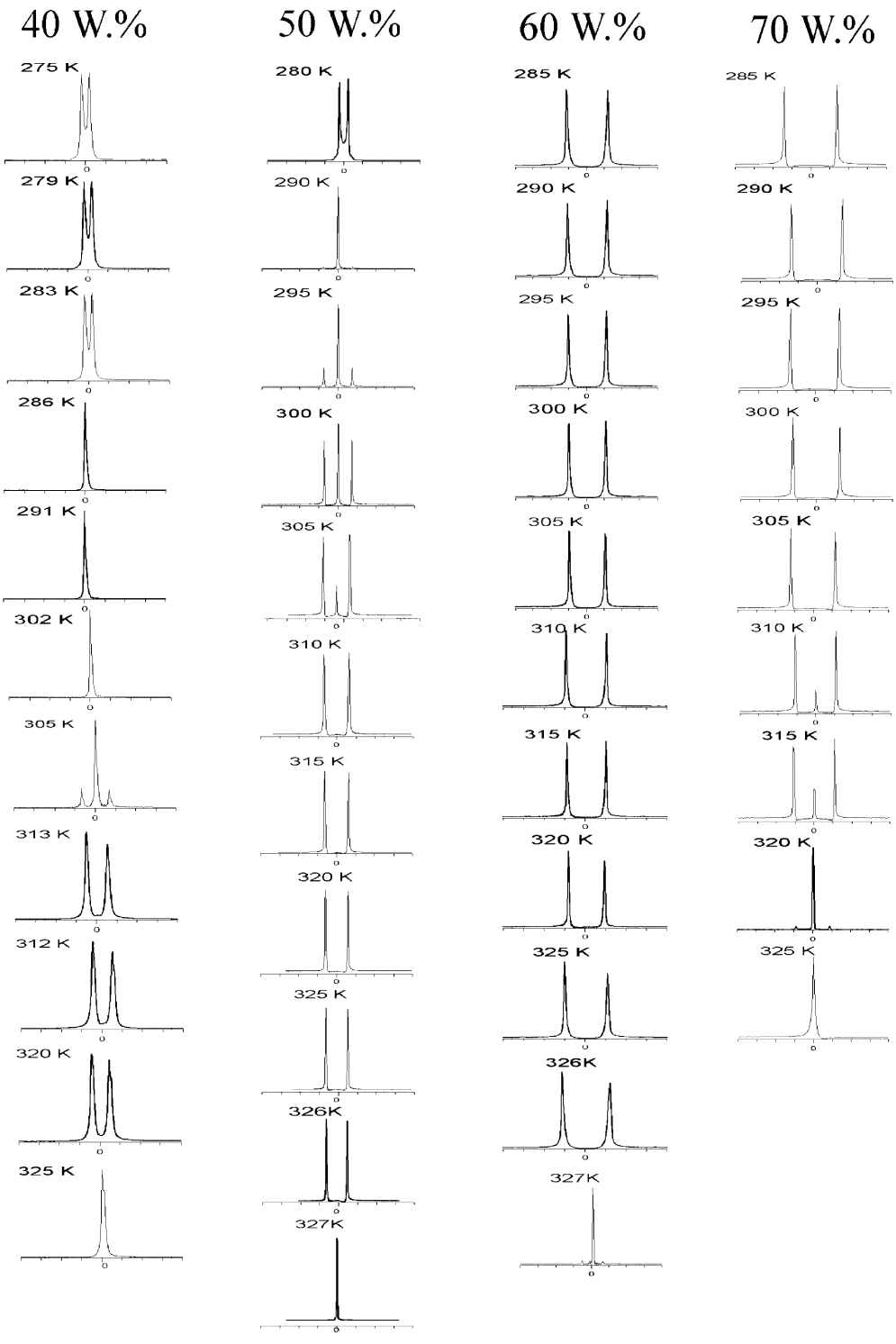

Fig. 6 ^{2}H-NMR spectra for different temperatures at concentrations of 40, 50, 60 and 70% (w/w) of M8GS11 surfactant

ally to a polymer backbone is commonly believed to strongly favor formation of nematic mesophases, or even to prevent ordering into smectic layers. On the other hand, the present polysoaps are made of rigid rod-like amphiphiles that should favor lyotropic smectic phases. This investigation should reveal if the synthesized polysoaps exhibit liquid crystalline phases in water, and if the lyotropic smectic layering is favored in water. Furthermore we want to analyze how the spacer length influences the identity and stability of the mesophases.

The phase behavior of the binary amphiphile/water solutions are studied by polarizing microscopy combined with ^{2}H-NMR measurements. The resulting ^{2}H-NMR spectra and liquid crystalline textures for the identification of the mesophases are presented for the monomeric compound **M8GS11** as an example. Its phase diagram will be also described in detail. Thereafter we will compare the phase behavior of the homologous series of monomeric and polymeric surfactants and conclude with a discussion about the chemical structure – phase behavior relationship of the investigated compounds.

Phase behavior of **M8GS11** in water

The phase behavior of the **M8GS11** surfactant was determined over a concentration range of 15–80% amphiphile (w/w). The phase diagram is shown in Fig. 4. The very concentrated and diluted regions have been extrapolated. At temperatures above the crystalline regions the monomer is miscible with water in a broad concentration range from 0% (w/w) to a maximum of 52% (w/w), depending on temperature. In analogy to other non-ionic oligo(ethylene glycol)-containing surfactants, **M8GS11** shows a miscibility gap with a lower critical consolution point at 32 °C. Against our expectations for rigid rod-like amphiphiles, the binary **M8GS11**/water system shows different lyotropic mesophases depending on surfactant concentration or temperature. The first mesophase appears in the concentration range from 30–55% (w/w) with T_{max} at 15.5 °C. This phase is identified by microscopic investigations as a hexagonal H_1 phase, on the basis of the characteristic optical fan-shaped textures (Fig. 5a). The second mesophase exists at higher temperatures and at surfactant concentrations from approximately 25–77% (w/w). Microscopic investigations identified this mesophase as a lyotropic smectic phase. Depending on the concentration range, two characteristic optical textures have been found for this mesophasic region: homeotropic areas with oily streaks at low concentrations (Fig. 5b) and focal conic at higher concentrations (Fig. 5c). The present focal conic textures exhibit high birefringence and are identical to those of smectic A thermotropic mesophases. Between the hexagonal and the lyotropic smectic mesophase no optical isotropic bicontinuous V_1 phase is found. To confirm microscopic investigations, ^{2}H-NMR measurements of defined surfactant/water mixtures were performed. This method allows an accurate determination of the biphasic regimes. Figure 6 shows the ^{2}H-NMR spectra for different temperatures at concentrations of 40, 50, 60 and 70% (w/w). For the samples with 40% (w/w) and 50% (w/w) of **M8GS11** we find a lyotropic to isotropic transformation between 288 K and 285 K, and an isotropic to lyotropic transformation between 293 K and 303 K. The mesophase at lower temperatures has approximately half the value of the quadrupole splitting at higher temperatures.

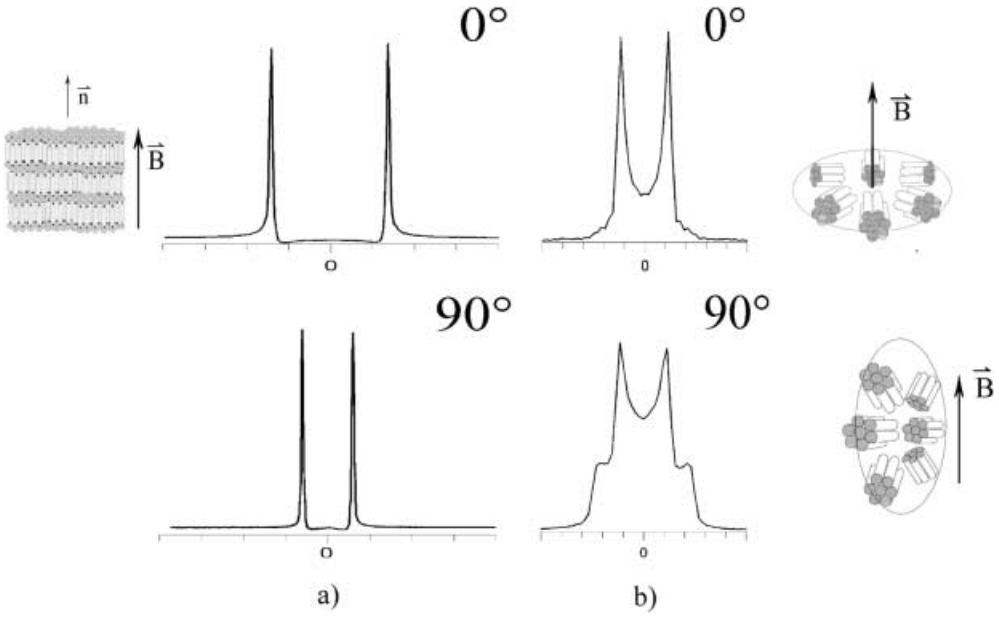

Fig. 7a,b ^{2}H-NMR spectra from aligned **a** lyotropic smectic sample of M8GS11 at 40% (w/w) and 8 °C, and **b** hexagonal sample of M8GS11 at 40% (w/w) and 13 °C rotated by 90° about an axis perpendicular to the magnetic field

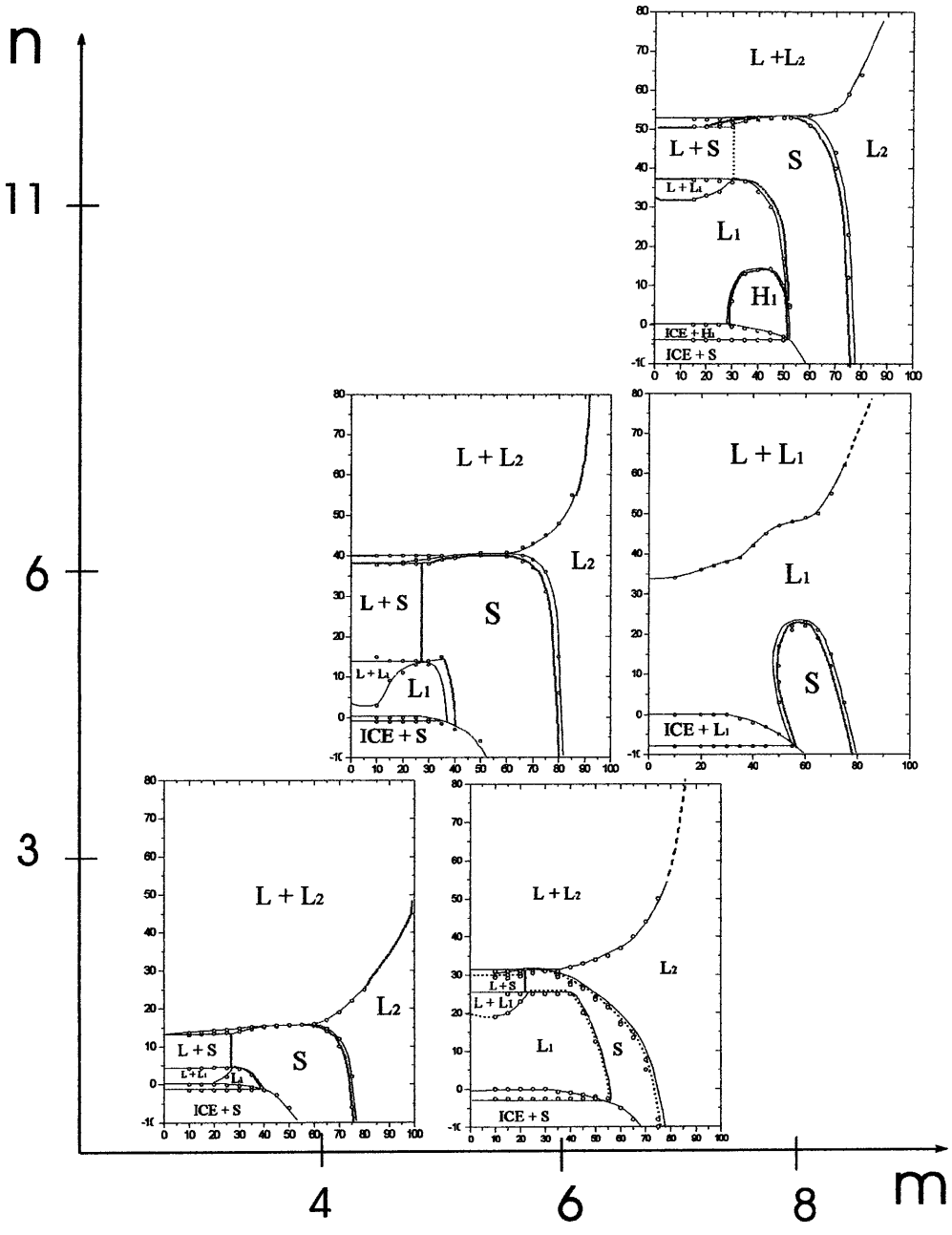

Fig. 8 Phase diagrams of low molecular weight surfactants

To identify the mesophase structure, orientation measurements at various angles to the magnetic field were performed. Figure 7 shows the spectra from the aligned lyotropic smectic sample (**M8GS11** at 60% (w/w) and 8 °C) and the hexagonal sample (**M8GS11** at 40% (w/w) and 13 °C) rotated by 90° about an axis perpendicular to the magnetic field. Due to the rigid aromatic core, the surfactant exhibits a strong positive anisotropy of the diamagnetic susceptibility and orientates parallel to the external magnetic field. The analysis of spectral line shapes of samples with director orientation at 0° (top spectra in Fig. 7) and 90° (bottom spectra in Fig. 7) to the magnetic field, confirms the existence of a hexagonal phase at lower surfactant concentrations and a highly ordered lyotropic smectic phase at 60% (w/w) surfactant. The line shape of the lyotropic smectic phase spectrum (left in Fig. 7) shows a doublet of narrow lines, and the quadrupole splitting decreasing to half the value at 90°. This is the evidence for a uniformly oriented sample with the director parallel to the magnetic field. Furthermore, the existence of a perfectly aligned lyotropic smectic phase has been confirmed by conoscopy and a regularization method [7]. The spectra at the right of Fig. 7 represent the sample in the

hexagonal phase with an inner and outer doublet, whose splitting is related by a factor of 1:2. This results from a planar director distribution of the cylindrical micelles with their axes perpendicular to the magnetic field.

Low molecular weight surfactants

The phase diagrams for the low molecular weight surfactants with different spacer-lengths (n) and hydrophilic chain-lengths (m) are displayed in Fig. 8. The transition temperatures (T_{max}) for the liquid crystalline phases and lower critical consolute temperatures (LCSTs) are summarized in Table 3. In the concentration range from approximately 35% to 70–80% (w/w) lyotropic smectic phases exist, except for **M8GS11**, where the hexagonal H_1 phase is additionally found, as mentioned before. The phase diagrams of the more rigid amphiphiles with smaller flexible groups ($n \leq 6$ and $m \leq 8$) given in the middle and bottom of Fig. 8, show no lyotropic polymorphism. The existence of the smectic phases can be clearly identified under the polarizing microscope. Figure 9 shows the focal conic textures between crossed polarizers observed for the surfactant **M6GS6** at 70% (w/w) and 24 °C. This texture, identical to that of thermotropic smectic A phases, have been found for all the rigid rod-like amphiphiles presented in this work at concentration ranges varying from 65% (w/w) to 75% (w/w). Only the **M8GS6** surfactant is soluble over the whole concentration range, forming the isotropic solution L_1. The L_1 regime is limited to concentration ranges between 0% (w/w) to a maximum of 55% (w/w) for the other more hydrophobic surfactants **M4GS3**, **M6GS3**, **M6GS6** and **M8GS11**. At high temperatures the lyotropic smectic phases are limited by a broad miscibility gap where two isotropic solutions ($L + L_2$) coexist. At temperatures below 0 °C pure water crystallizes and coexists with the isotropic phase or mesophase. For the pure surfactants, no crystallization is observed.

Side-on amphiphilic polymers

The phase diagrams for the polymers with different spacer-lengths (n) and hydrophilic chain-length (m) are displayed in Fig. 10. The transition temperatures (T_{max}) and the glass transition temperatures are summarized in Table 4. The four side-on polymers exhibit only lyotropic smectic phases in water, extended from concentrations of about 20–40% to a maximum of 80% (w/w). No hexagonal phase and only a lyotropic smectic mesophase are observed for the **P8GS11** polymer. The ^{2}H-NMR measurements at various angles and for a low **P8GS11** concentration of 35% (w/w) are displayed in Fig. 11. The spectra show an inner single peak that corresponds to unoriented domains with defects in the lyotropic smectic structure near to the isotropic L_1 phase. The outer doublet of the spectra varies its splitting when rotating the sample about an axis perpendicular to the magnetic field. The 90° spectra at the bottom of Fig. 11 has half the splitting of the 0° spectra at the top. These observations confirm the existence of the lyotropic smectic phase at low amphiphilic concentrations and near to the isotropic L_1 region.

All lyotropic smectic phases are followed at higher temperatures by a broad miscibility gap $L + L_2$. The solubility of the **P6GS6** polymer in water is limited to a narrow concentration range between approximately 20% and 30% (w/w). The hydrophobic **P4GS3** polymer shows a solubility between 25% and 30% (w/w), while the more hydrophilic polymers **P6GS3** and **P8GS11** exhibit an isotropic L_1 solution below approximately 15 °C in a concentration range of 0% to 30–35% (w/w). For the pure polymers no crystallization was observed and the glass transition temperatures are located between a maximum of −37 °C for the **P4GS3** polymer and a minimum of −56 °C for the **P8GS11** polymer.

In the synthesized homologous series of low molar mass surfactants, the molecular rigidity, i.e. the grade of rod-like shape exhibited by the amphiphile molecules, has systematically been varied. Since the rigid aromatic core represents the rigidity of the molecule, variation of the spacer and/or ethylene glycol chain length yields different levels of molecular flexibility. For the molecules

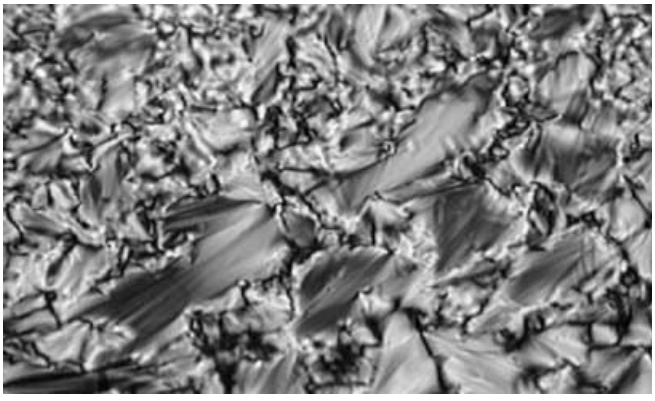

Fig. 9 S_A focal conic texture of M6GS6 at 70% (w/w) and 24 °C

Table 3 Transition temperatures and lower critical consolute tempearatures (*LCST*) for the monomers. *S-i* Smectic-isotropic

Monomer	LCST (°C)	S-i (°C)	H_1 (°C)
M4GS3	< 0	16	–
M6GS3	18	31	–
M6GS6	3	40	–
M8GS6	34	23	–
M8GS11	32	54	15.5

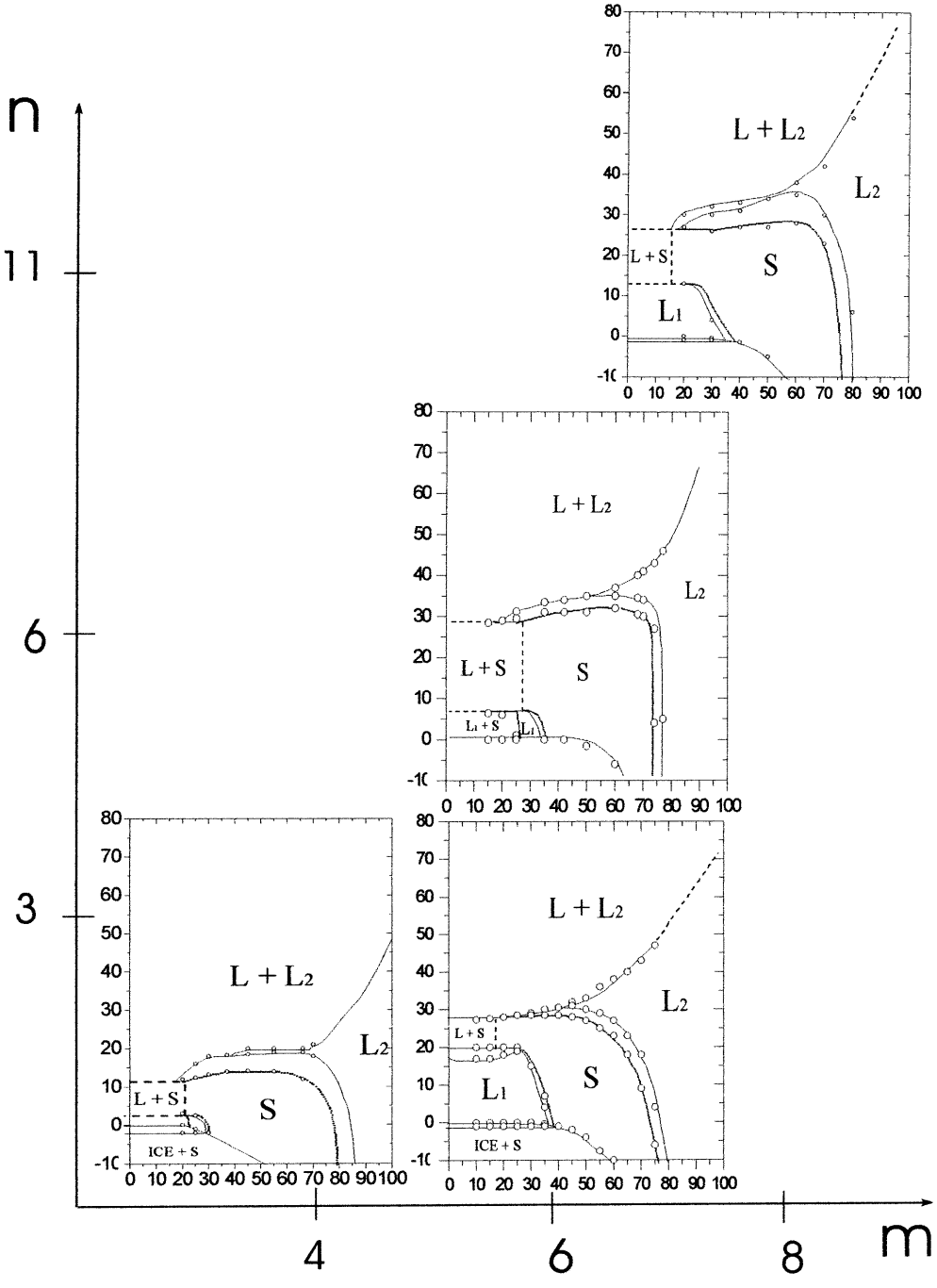

Fig. 10 Phase diagrams of side-on amphiphilic polymers in water

Table 4 Glass transition temperatures (*Tg*) and clearing temperatures for the side-on polymers

Polymer	*Tg* (°C)	S-i (°C)
P4GS3	−37	20
P6GS3	−46	33
P6GS6	−50	35
P8GS11	−56	34

M6GS6 and **M8GS11** we found very different phase behavior although these two systems have nearly the same hydrophilic/lipophilic balance. The phase diagram of **M6GS6** with only a lyotropic smectic phase in a broad concentration range is derived from a packing constraint of this amphiphile to disk-shape micelles. The flexible system **M8GS11**, with the longest spacer and hydrophilic ethylene oxide chains, shows, in addition to the lamellar phase, a hexagonal phase. Furthermore, **M8GS6**, which is more hydrophilic than **M8GS11**, does

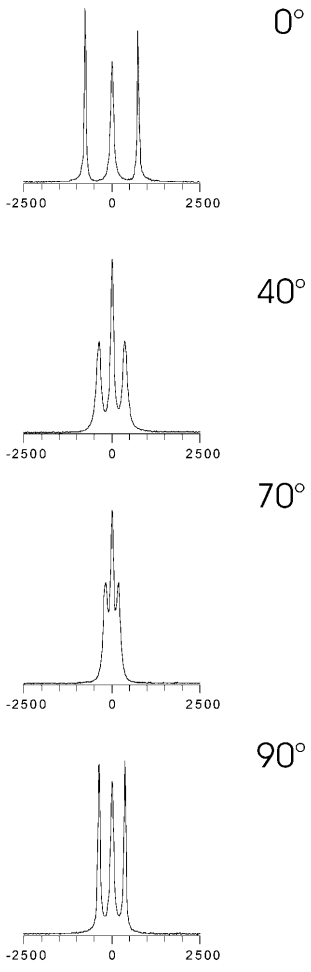

Fig. 11 ^{2}H-NMR spectra of partial oriented (outer doublet corresponds to the oriented lamellar domains; inner single peak corresponds to unoriented domains) P8GS11/water sample at 35% (w/w) and 28 K. The spectra were obtained by slow cooling of the sample in the magnet from the isotropic phase and rotating about an axis perpendicular to the magnetic field

not exhibit a hexagonal or cubic phase. According to the polymorphism of classical non-ionic aliphatic ethylene glycol amphiphiles, increasing the hydrophilicity of the surfactants supports the formation of cubic and hexagonal phases, while lamellar phases are preferentially exhibited by systems with small hydrophilic head groups and long aliphatic chains. This means, the HLB of those molecules is decisive for the formation of different micelle shapes at different concentrations and temperatures. In the case of the amphiphiles presented in this paper, the HLB does not influence the lyotropic polymorphism. Only the molecular geometry constitutes a critical parameter for the shape of the micelles.

By comparing the phase diagrams of these surfactants with those of their side-on polymer analogs, we find another important factor that determines the extension of the lyotropic mesophase with respect to temperature: the spacer length. The smectic lyotropic phase consist of surfactant monolayers [6], instead of bilayers, which are normally found in lamellar phases [16]. Considering that the micellar packing in water has to be consistent with the molecular geometry of the amphiphiles linked to the polymer, the thickness of the hydrophobic layer is limited by the length between the two hydrophilic end groups terminally attached to the rigid aromatic core. Within this hydrophobic layer, three different polymer moieties coexist: the rod-like aromatic core, the aliphatic spacer and the polysiloxane backbone.

Compared to the analogous monomer, the polymers **P4GS3** and **P6GS3** with three methylene groups as spacer, favor the formation of the lyotropic smectic phase with respect to concentration and temperature. The extension of the lyotropic smectic phase in the **P6GS6** polymer with the hexenyl spacer gets broader with respect to concentration, but it decreases by 5° with respect to temperature compared to **M6GS6**. A decrease of 20° for the smectic to isotropic phase transformation temperature is found for the **P8GS11** polymer, which has a long undecenyl-spacer. All these observations give evidence for the strong dependence of the mesophase stability on the spacer length. A possible explanation for this phenomenon might be a partial suppression of the ethylene glycol hydration with water by the polymer backbone. The length of the spacer determines the main chain flexibility as indicated by the different glass transition temperatures. The more flexible **P8GS11** polymer is able to adopt a less pronounced anisotropic main chain conformation, which leads to defects in the lamellar structure. These defects might disturb the hydrophilic areas and consequently vary the hydrophilic/hydrophobic equilibrium established in the analog **M8GS11** monomer. The ^{2}H-NMR spectra with the inner single peak given in Fig. 11 point towards this explanation and show the defects in the lyotropic smectic layering of **P8GS11**.

To conclude, in the present work we have synthesized lyotropic liquid crystalline side-on polymers, in which only lamellar association of the micellar solutions occurs. The changes in mesophase behavior with related monomers caused by the analogous lateral polymer addition of side-on surfactants cause a destabilization of columnar association and a stabilization of the lyotropic smectic mesophases, depending on spacer-length. The extension of the regions of the mesophase with respect to amphiphilic concentration increases.

References

1. Keller-Griffith R, Ringsdorf H, Vierengel A (1986) Coll Polym Sci 264:924
2. Ringsdorf H, Schlarb B, Venzmer J (1988) Angew Chem 100:117
3. Lindner N, Köbel M, Sauer C, Diele S, Jokiranta J, Tschierske C (1998) J Phys Chem B 102:5261
4. Lee M, Cho B, Zin H (1998) Angew Chem Int Ed Eng 37:638
5. Boden N, Bushby RJ, Hardy C (1985) J Phys Lett 46:325
6. Schafheutle MA, Finkelmann H (1988) Liq Cryst 3:1369
7. Jahns E, Finkelmann H (1987) Colloid Polym Sci 265:304
8. Hardoin F, Mery S, Achard M, Mauzac M, Davidson P, Keller P (1990) Liq Cryst 8:564
9. Arehart SV, Pugh C (1997) J Am Chem Soc 119:3027
10. Ward A, Ku H, Phillippi MA, Marie C (1988) Mol Cryst Liq Cryst 154:55
11. Schnepp W, Disch S, Schmidt C (1993) Liq Cryst 14:843
12. Winterhalter J, Maier D, Grabowski DA, Honerkamp J, Müller S, Schmidt C (1999) J Chem Phys 110:4035
13. Kratzat K, Finkelmann H (1994) Colloid Polym Sci 272:400
14. Blackburn JC, Kilpatrick PK (1992) Langmuir 8:1679
15. Lecommandoux S, Achard MF, Hardouin F (1998) Liq Cryst 25:85
16. Smith GS, Clark NA (1990) J Chem Phys 92:4519